Molecular ion transport mechanism of dental enamel formation
FINAL SCIENTIFIC REPORT

Dental enamel, the hardest mammalian tissue, is produced by ameloblasts. During tooth formation, these cells are in close functional contact with mesenchymal stem cells to differentiate and then produce the teeth, consisting of the enamel outside, while the dentin inside. The major disorders of enamel originate from environmentally dependent and genetic conditions. Among these, molar incisor hypomineralization, dental caries, dental fluorosis and mutation of certain key proteins are the most prominent ones.

Ameloblasts show many similarities to other transporting epithelia although their secretory product, the enamel matrix, is quite different. Ameloblasts originating from epithelial stem cells, and actually also mesenchymal stem cell originated odontoblast direct the formation of hydroxyapatite crystals, which liberate large quantities of protons that then need to be buffered to allow mineralization to proceed. Buffering requires a tight pH regulation and secretion of bicarbonate by ameloblasts. Many investigations have used immunohistochemical and knock-out studies to determine the effects of these genes on enamel formation, but up till recently very little functional data was available for mineral ion transport.

To address this, we developed novel 2D and 3D in vitro models using HAT-7 ameloblast cells, and also cells from rat incisors and investigated the molecular physiology and pathophysiology using these novel experimental models. Our investigations aimed to address the molecular mechanisms leading normal or disturbed amelogenesis. Understanding the largely unknown molecular pathophysiology of the multistep ion transport process may help to develop multi-step nanotechnological strategies to renew enamel.

Optimization of HAT-7 cultures to enhance the applicability of our novel, two dimensional, functional in vitro ameloblast model

During enamel maturation, ameloblasts have crucial role in mineral transport and bicarbonate secretion to neutralize excess protons liberated during hydroxyapatite formation. There have been no functional data existed for mineral ion transport by ameloblasts. Therefore, we aimed to further develop and optimize our novel in vitro model using the HAT-7 rat ameloblast cells (Bori et al. J Dent Res, 2016) to functionally study epithelial ion transport during amelogenesis . To obtain monolayers, HAT-7 cells were cultured in various culture media for 1-7 days on Transwell membranes. The expression of ion transporters and tight junction proteins was investigated by quantitative RT-PCR. We monitored transepithelial resistance as an indicator of tight junction formation and polarization. We also evaluated intracellular pH changes by microfluorometry using BCECF fluorochrome. The activites of specific bicarbonate and chloride transporters, anion exchangers were tested using selective transporter inhibitors.

In these optimized conditions HAT-7 cells formed polarized epithelia on permeable supports in all tested culture media tested, but the DMEM-F12 medium containing 2.1 mM calcium and 10^{-8} M dexamethasone yielded the best reproducible results. HAT-7 cells expressed various claudins and the ion transporters previously found in ameloblasts. We detected the basolateral activity of sodium-proton exchange by NHE transporter, using amiloride. Basolateral anion exchanger and NKCC activities were also demonstrated applying DIDS and bumetanide. High apical membrane CO_2 permeability and substantial basolateral bicarbonate uptake (which was sensitive to Na^+ withdrawal) were inhibited by the carbonic anhydrase inhibitor acetazolamide and by H_2DIDS inhibition. Measurements of transepithelial bicarbonate transport showed a marked increase in response to ATP and forskolin.

In conclusion, we succeeded to optimize the culture and functional test conditions to evaluate the formation of polarized monolayers by transepithelial resistance and the enhanced activity of ion transporters affecting pH regulation and vectorial bicarbonate transport in the ameloblast originated cells.

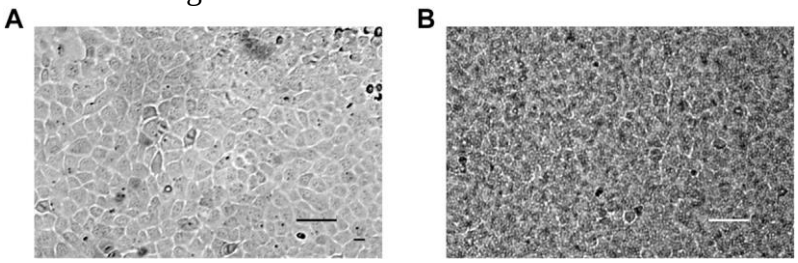

Morphology of 2D HAT-7 cell cultures. (A) HAT-7 cells grown in control medium as a conventional monolayer on plastic in a T-25 culture flask for 3 days. (B) HAT-7 cells grown in differentiation medium as a polarized monolayer on a Transwell permeable support for 7 days. Also visible are the 0.4 μm pores in the polyester supporting membrane. Scale bars: 100 μm.

Three-dimensional organization of ameloblast originated cells – organoid-like structures

After optimizing experimental conditions for our 2D model, we aimed to achieve three-dimensional (3D) growth of HAT-7 cells on showing organoid-like organization and reticular networks depending on the concentration of the applied Matrigel/BME scaffold in both HAT-7 cells and primary cultures from rat incisor cervical loop, just like we did before using salivary gland epithelial cells.

Our aims were to optimize the culture conditions for the three-dimensional growth of ameloblast-derived HAT-7 cells and to test the effect sof fluoride exposure on HAT-7 spheroid formation. To generate 3D HAT-7 structures, cells were dispersed and plated within a Matrigel extracellular matrix scaffold and incubated in three different culture media. Spheroid formation was then monitored over a two-weekperiod. Ion transporter and tight-junction protein expression was investigated by RT-qPCR. Intracellular Ca2+ and pH changes were measured by microfluorometry using the fluorescent dyes fura-2 and BCECF.
A combination of Hepato-STIM epithelial cell differentiation medium and Matrigel induced the expansion and formation of 3D HAT-7spheroids. The cells retained their epithelial cell morphology and continued to express both ameloblast-specific and ion transport-specific marker genes. Furthermore, like two-dimensional HAT-7 monolayers, the HAT-7 spheroids were able to regulate their intracellular pH and to show intracellular calcium responses to extracellular stimulation. Finally, we demonstrated that HAT-7 spheroids may serve as a diseasemodel for studying the effects of fluoride exposure during amelogenesis.

In conclusion, HAT-7 cells cultivated within a Matrigel extracellular matrix form three-dimensional, multi-cellular, spheroidal structures that retain their functional capacity for pH regulation and intracellular Ca^{2+} signaling. This new 3D model will allow us to gain a better understanding of the molecular mechanisms involved in amelogenesis, not only in health but also in disorders of enamel formation, such as those resulting from fluoride exposure.

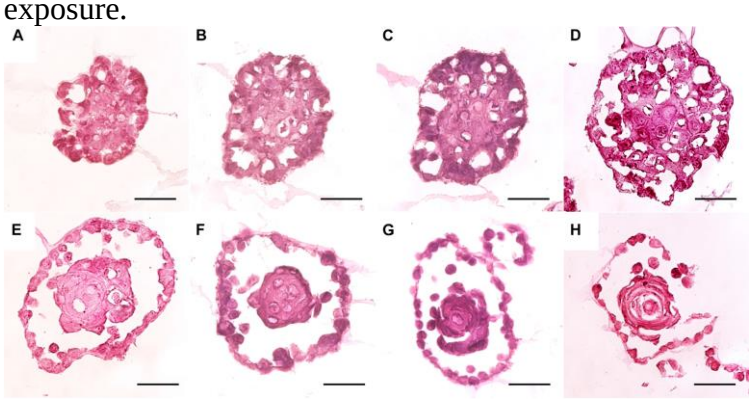

Histology of HAT-7 spheroids grown for 7 days in Matrigel with Hepato-STIM medium. Spheroids were isolated from the matrix using 0.25% trypsin/ EDTA. Frozen sections (5 μm) were stained with haematoxylin and eosin. Scale bars: 50 μm.

Culturing and scaling up progenitors of dental origin using microcarriers

Mesenchymal and epithelial progenitors of dental origin, including dental pulp stem cells are promising sources for cell therapy, tissue engineering, drug discovery and disease modeling due to their accessibility and capability of multi-lineage differentiation. There is an urgent need to develop effective, reproducible and safe scaling-up methods producing large amount of therapeutically active cells. Microcarrier based culturing in bioreactors and similar dynamic systems is a promising technology combining a required large growth surface area with an automated process control.

We tested the suitability of two well characterized microcarriers, non-porous Cytodex 1 and porous Cytopore 2, for culturing dental originated stem cells using a shake flask system. Human, isolated dental stem cells were cultured on these microcarriers in 96 well plates, and further expanded in shake flasks for upscaling experiments. Cell viability was measured using the Alamar Blue assay, while cell morphology was observed by conventional and two-photon microscopies. Glucose consumption of cells was detected by the glucose oxidase/Clark-electrode method. Cells adhered to, and grew well on both microcarrier surfaces and were also found in the pores of Cytopore 2. Cells grown in tissue culture plates (static, non-shaking conditions) yielded $7*10^5$ cells/well. In shake flasks, static preincubation promoted cell adhesion to microcarriers. Under dynamic culture, in shaking conditions approximately two magnitudes higher cell yield can be obtained in shake flasks. Our data also glucose supply from the medium by day 7 even with partial We also found that batch-feeding by glucose is absolutely important for high cell yield. In conclusion both non-porous and porous microcarriers are suitable for upscaling DPSCs under dynamic culture conditions.

The use of bioreactors and similar systems may provide a safe and effective technology to supply routine cell therapeutic applications. Monitoring glucose consumption is important to optimize culturing parameters of epithelial and mesenchymal progenitor cells grown in bioreactors.

Isolation, culture and characterization of primary epithelial cells from rat incisors and investigations on ameloblasts in rat incisor tissue slices

Constantly growing rodent incisors are suitable to model ameloblast activity. We aimed to develop methods to reliably dissect enamel organs, isolate and cultivate epithelial ameloblast progenitors, and also secretory stage and maturation ameloblast cells. We utilized technologies that we previously developed for isolating and culturing salivary epithelial cells (Hegyesi et al, Tissue Engineering, 2015). Wistar rats were euthanized. After mandible removal, the tissues surrounding lower incisors were aseptically eliminated and the epithelial side was scraped off in three different regions: at the basis to obtain cervical loop epithelial progenitors, at the lower region secretory ameloblasts, and at the upper region maturation ameloblasts, respectively. Afterwards, cells were incubated in a collagenase/dispase containing HBSS solution, while gently pipetted up and down, then filtered to get rid of debris and obtain isolated epithelial cells. The three different cell cultures were cultivated in Hepato-STIM medium in plastic dishes, while their growth was monitored. Finally cells were fixed for light microscopic evaluations and immunocytochemistry.

We successfully isolated epithelial cells from both the cervical loop, and the secretory, and also the maturation ameloblast regions of the rat incisor. Isolated cervical loop region cells were cultivated and passaged. These cells show epithelial morphology and characteristics, and the lack of mesenchymal cell characteristics. They were able to form 3D structure when cultivated high on laminin-containing, growth factor-reduced Matrigel. On the other hand, cells isolated from the secretory and maturation ameloblast regions exhibit no or rather

moderate cell proliferation and epithelial patch formation activities. In conclusion, the newly developed isolation and cultivation methods serve to model the proliferation and differentiation capacity of ameloblast. These epithelial cultures are used in molecular physiology studies, which indicate that these cultures exhibit similar ion transport processes as the HAT-7 ameloblast model.

We also set up the system to investigate ameloblasts in situ on isolated rat incisor preparations having living ameloblast monolayers on the enamel surface. Unfortunately, electrophysiological and microfluorometry data obtained using that system are very heterogeneous and hardly reproducible. Therefore, we decided that the primary models to use were the primary cells isolated and cultivated from the enamel formation surface of rat incisors.

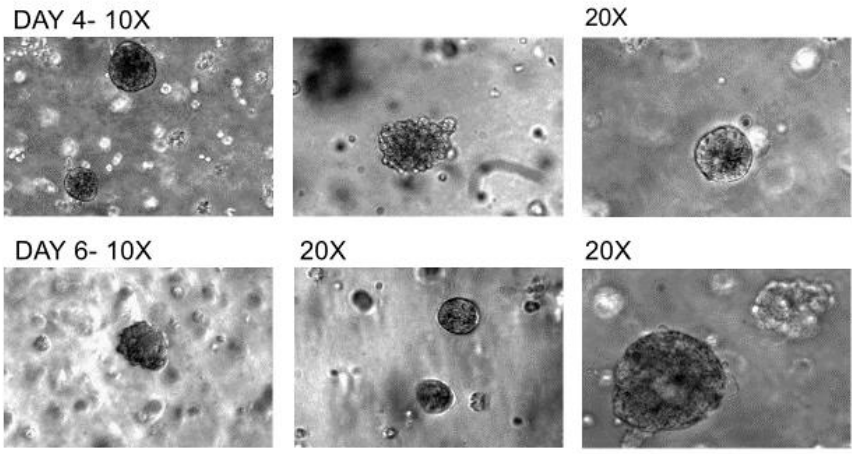

Speroid culture of ameloblast-like cells isolated from rat cervical loop. The figure shows spheroids with different magnifications, 4 and 6 days after cultivation in Matrigel using HepatoSTIM medium. These speroids could be isolated, cells dissected and recultivated again in Matrigel to obtain a large number of shperoids.

Significance of intracellular and extracellular pH regulation and extracellular pH cyclization in amelogenesis

The process of amelogenesis is well understood at the histomorphological level, but the regulation of crystal formation and the underlying molecular mechanisms are still largely unknown. Ameloblast cells derived from the oral epithelium regulate enamel maturation. In addition to the secretion of matrix proteins and the transport of minerals, pH regulation is also essential as the formation of hydroxyapatite crystals generates large quantities of H^+ ions, which must be neutralized by the secretion of HCO_3^-.

Our studies revealed that the dental enamel producing ameloblasts, the pancreas and the salivary glands have marked developmental, structural and functional similarities. One of the most striking similarities is their bicarbonate-rich secretory product serving acid neutralization. Interestingly, the ion and protein secretion by the pancreas, the salivary glands, and maturation ameloblasts are all two-step processes, of course with significant differences too. As they all have to defend against acid exposure by producing extremely large quantities of bicarbonate, the failure of this function leads to deteriorating consequences. We characterized the defense mechanisms of the pancreas, the salivary glands and enamel-producing ameloblasts against acid exposure and compared their functional capabilities to do this by producing bicarbonate. We published our developed concept on this and also our related in leading high impact journals of the field.

During the maturation phase, the phenomenon of pH cycling is of paramount importance. Genetic or environmental impairment of transport and regulatory leads to enamel defects. To explore these processes, we have developed an *in vitro* model suitable for functional studies. Central elements of this model are that differentiated ameloblast-derived

cells cultured on a permeable membrane express ameloblast-specific protein markers, form tight junctions, become functionally polarized, and are capable of vectorial HCO_3^- secretion. The results of our own experimental work led to a new, complex model involving ion transporters and ion channels contributing to the molecular mechanism of pH cycling of ameloblast cells.

Related to this, currently we carried out cell physiological experiments to demonstrate the direct triggering activity of extracellular, apical pH decrease on bicarbonate secretion in polarized HAT-7 cells. This work led to the discovery that the development of functional 2D layers of ameloblast originated cells lead to the polarization which is clearly shown by our observation that acidification leads to fundamentally different intracellular pH changes between the basolateral and the apical side of the cells. This observation gives the fundament of pH cycling, which is achieved and regulated by maturation ameloblast leading to the hardest mineralized tissue in mammalians, the dental enamel.

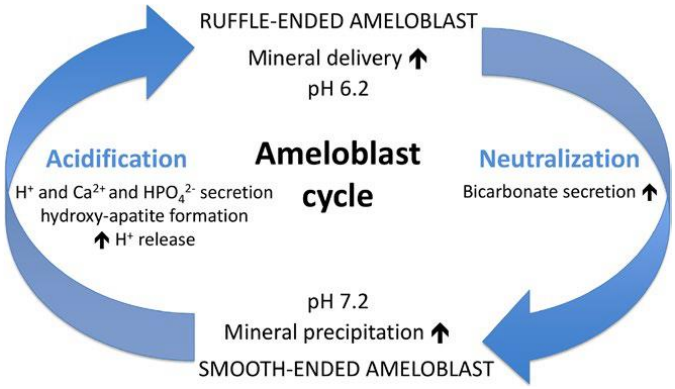

pH cycle in the luminal surface of ameloblasts during the maturation phase of amelogenesis. Cells cycle between smooth-ended and ruffle-ended stages multiple times. This cycling is accompanied by luminal pH changes between approximately 6.2 and 7.2. The primary driver of acidification is the release of protons liberated during hydroxyl-apatite formation. Acidification is counterbalanced then by the buffering effect of bicarbonate (Rácz et al, 2021)

Differential basolateral and apical AE and NKCC activities demonstrate polarization of ameloblast cells

A coordinated transport of chloride and bicarbonate ions is required for enamel maturation during amelogenesis. We compared the apical and basolateral HCO3-/Cl- anion-exchanger (AE) and sodium-potassium-chloride cotransporter (NKCC) activities in HAT-7 cells. To obtain monolayers, HAT-7 cells were cultured in differentiation medium for 4 days on Transwell membranes. We monitored transepithelial resistance as an indicator of tight junction formation and polarization. We evaluated intracellular pH changes by microfluorometry using BCECF fluorochrome. The activity of transporters was tested by specific inhibitors.

In HAT-7 cells grown on Transwell, the basolateral AE activity was high, and could be inhibited by DIDS. On the other hand, AE activity was very low at the apical side, and not significantly affected by DIDS. Additionally, we found a substantial NKCC activity in HAT-7 cells indicated by the rapid decrease of intracellular pH after an alkaline load. This activity was substantially inhibited by basolateral bumetanide administration, but not by apical bumetanide, indicating the presence of NKCC activity only at the basolateral but not at the apical side of the ameloblast originated cells. In conclusion, we identified differential, side-specific, localized activities of AE and NKCC transporters in HAT-7 ameloblast cells, polarized on Transwell membranes.

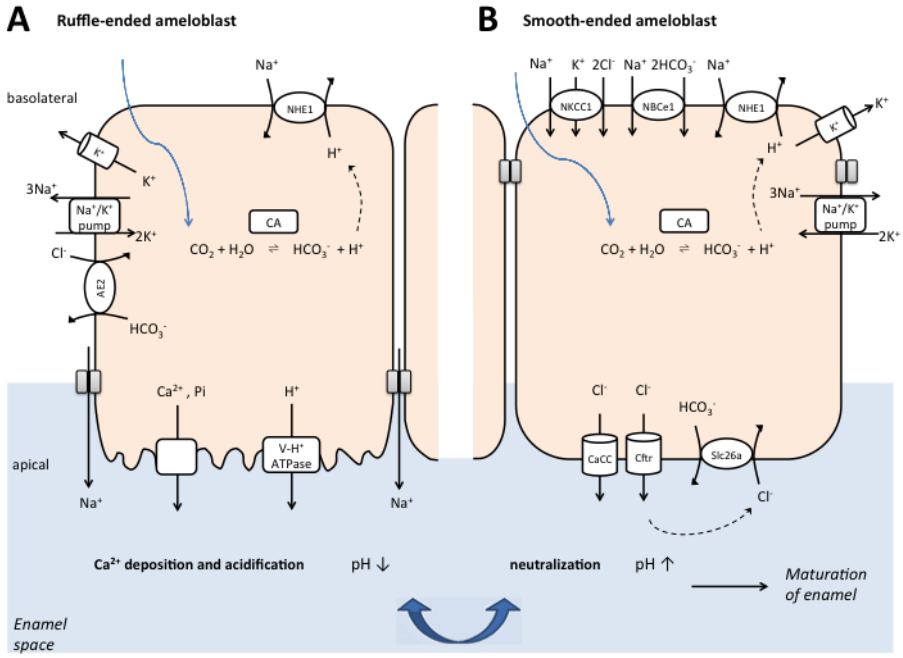

Simplified model depicting bicarbonate and electrolyte secretion in ruffle-ended and smooth-ended ameloblast cells. The bottom of the figure shows that ameloblasts secrete bicarbonate to neutralize acidity in the mineralizing enamel space. (A) Ruffle-ended ameloblast cells secrete Ca^{2+} and phosphate ions into the enamel space. Ca^{2+} is mostly taken up by the store-operated calcium entry pathway basolaterally and transported out of the cells at the apical pole by NCKX4 and NCX exchangers. Phosphate transport probably occurs via Na+-dependent phosphate (Pi) transporters. The pH is slowly decreasing during mineralization because a great quantity of protons liberated during the formation of hydroxyapatite crystals and also, probably by an active process, the apical activity of V-type H^+ ATPases.
(B) Smooth-ended ameloblast cells reorganize the tight junctions to neutralize luminal acidity in the enamel space by bicarbonate. Intracellular bicarbonate accumulation is facilitated by the basolateral electrogenic Na+/ HCO3− cotransport and by carbonic anhydrase supported by proton extrusion through Na+/H+ exchangers. The main mechanism of intracellular Cl^- accumulation is probably the activity of $Na^+/K^+/Cl^-$ cotransporter driven by the Na^+/K^+ ATPase generated Na+ gradient. Apically, Cl^- and to a loss extent bicarbonate leave the ameloblasts via both cAMP activated CFTR and Ca^{2+} activated chloride-channels. Bicarbonate can also be exchanged to already secreted Cl^- at the apical side by SLC26A exchangers. The cyclical changes from ruffle-ended to smooth-ended cell morphology and the ability to modulate pH in the enamel space ultimately allow the continuous expansion of hydroxyapatite crystal formation to reach an extremely high level of mineralization. (Rácz et al, 2018)

Ca^{2+} and Mg^{2+} homeostasis of ameloblast cells: the role of TRPM7 channel and TRPM7 channel-mediated pH-sensitive calcium transport

TRPM7 is a divalent-cation-permeable channel, with serine/threonine protein kinase activity, which plays an important role in Ca^{2+} and Mg^{2+} homeostasis in various cell types. TRPM7 channels are expressed in ameloblasts an d, in the absence of TRPM7, dental enamel is hypomineralized. TRPM7 channels are sensitive to intracellular Mg^{2+} and pH, and pH modulation is a key factor in ameloblast-mediated enamel mineralization. Here we have used again the HAT-7 rat ameloblast cell line to examine the possible role of the TRPM7 channel, and its pH sensitivity, in amelogenesis.

Transmembrane ion currents in HAT-7 cells were measured by patch-clamp electrophysiology in whole-cell configuration, in the presence of different intracellular Mg^{2+} concentrations, and in response to TRPM7 activators (mibefradil and naltriben) and inhibitors (NS8593 and FTY720). Changes in intracellular Ca^{2+} concentration ($[Ca^{2+}]_i$) and pH (pH_i) were measured using membrane-permeable fluorescent dyes. The cells showed strong TRPM7 mRNA and protein expression. Characteristic TRPM7 transmembrane currents were observed, which increased in the absence of intracellular Mg^{2+} ($[Mg^{2+}]i$), were reduced by elevated [Mg2+]i, and were inhibited by the TRPM7 inhibitors NS8593 and FTY720. Mibefradil evoked similar currents, which were suppressed by elevated $[Mg^{2+}]i$, reducing

extracellular pH stimulated transmembrane currents, which were inhibited by FTY720.Naltriben and mibefradil both evoked Ca^{2+} influx, which was further enhanced by the acidic intracellular conditions. The SOCE inhibitor BTP2 blocked Ca^{2+} entry induced by naltriben but not by mibefradil.

Decreasing extracellular pH stimulated a similar increase in outward current, which was inhibited by FTY720. Both mibefradil and naltriben evoked increases in $[Ca^{2+}]_i$ which were largely dependent on extracellular Ca_{2+}. Acidic intracellular conditions enhanced the TRPM7-mediated $Ca^{2+}{}_+$ influx.

Taken together, in HAT-7 cells, TRPM7 may serves both as a potential modulator of Orai-dependent Ca^{2+} uptake and as an independent Ca^{2+} entry pathway sensitive to pH. Therefore, we propose that TRPM7 contribute directly to transepithelial Ca^{2+} transport in amelogenesis.

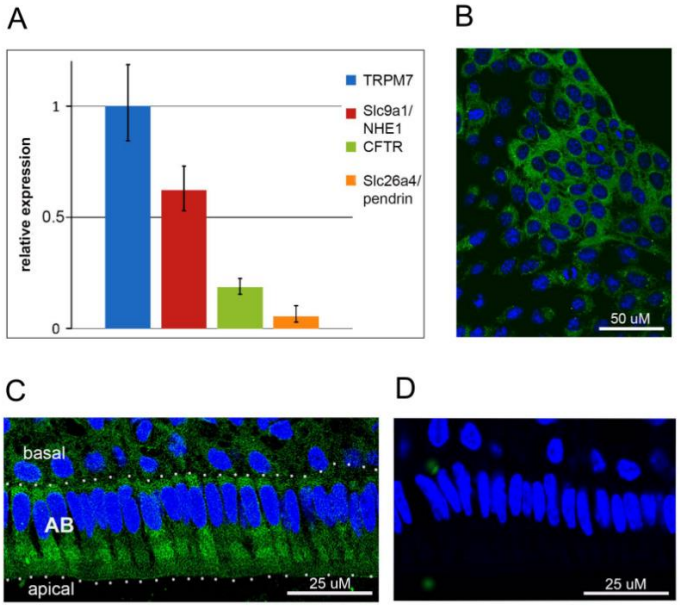

Expression of TRPM7 in HAT-7 cells and mouse incisor ameloblasts. (A) RT-of the mRNA expression levels of TRPM7, Slc9a1/NHE1, CFTR and Slc26a4/pendrin to mean TRPM7 expression in HAT-7 cells. (B,C) Immunolocalization of TRPM7 in HAT-7 cells (B,C) and mouse incisor ameloblasts (D.) (Kádár et al, 2021)

Functional presence of chloride channels in ameloblasts

During tooth enamel formation, besides Ca^{2+} and bicarbonate, ameloblasts also achieve the transport of $Cl^-$and PO_4^{3-} ions through tightly regulated processes, but not enough is known about this complex regulation.

Therefore, we aimed to select certain chloride channels presumably involved in enamel mineralization based on knock-out mouse model. We used the patch clamp electrophysiological method in whole cell configuration in HAT-7 cells and also in cells isolated and cultivated from a rat incisors. Besides being able to demonstrate the presence of functional, pH-dependent TRPM7 involved in Ca^{2+} transport, we also sought for channels of chloride ion transport and also the type of channels are involved in the regulation of Cl permeability. We investigated the function of Ca^{2+}-activated Cl- ion channels (CaCC) and also cAMP-activated CFTR chloride ion channels in these cells, but our results did not show a significant difference so far between them. Therefore, further studies are needed by methodological optimizations to identify the main chloride ion movement pathway in this cells.

Fluoride and other harmful agents in 2D and 3D culture conditions on ameloblast originated cells

At the maturation phase of amelogenesis, the phenomenon of pH cycling is of paramount importance, during which a rearrangement of tight-junctions can also be observed. Genetic or environmental impairment of transport and regulatory processes (e.g. dental fluorosis) leads to the development of enamel defects. To explore these processes, we have developed an in vitro model suitable for functional studies. Central elements of this model are that differentiated ameloblast-derived cells cultured on a permeable membrane express ameloblast-specific protein markers, form tight junctions, become functionally polarized, and are capable of vectorial HCO_3^- secretion.

The results of our own experimental work contribute to a better understanding of the molecular mechanism of pH cycling of ameloblasts. To investigate the mechanism of action of fluoride and other harmful, first HAT-7 cells were cultured 2D on Transwell permeable filters. We monitored transepithelial resistance (TER) as an indicator of tight junction formation and polarization. We evaluated intracellular pH changes by microfluorometry using the fluorescent indicator BCECF. Activities of ion transporters were tested by withdrawal of various ions from the bathing medium, by using transporter specific inhibitors, and by activation of transporters with forskolin and ATP. Cell survival was estimated by Alamar Blue assay. Changes in gene expression were monitored by qPCR. Bicarbonate secretion by HAT-7 cells was not affected by acute fluoride exposure over a wide range of concentrations. However, tight-junction formation was inhibited by 1 mM fluoride, a concentration which did not substantially reduce cell viability, suggesting an effect of fluoride on paracellular permeability and tight-junction formation. Cell viability was only reduced by prolonged exposure to fluoride concentrations greater than 1 mM.

As HAT-7 cells are able to accumulate bicarbonate ions from the basolateral to the apical fluid spaces, we propose that in the future the HAT-7 2D system along with similar cellular models will be useful to functionally model ion transport processes during amelogenesis. Additionally, we also suggest that similar approaches will allow a better understanding of the regulation of the cycling process in maturation-stage ameloblasts, and the pH sensory mechanisms, which are required to develop sound, healthy enamel. Since the exposure to 1 mM fluoride has little effect on bicarbonate secretion or cell viability but delays tight-junction formation, suggesting a fundamentally novel mechanism that may contribute to dental fluorosis. Under our experimental conditions, dexamethasone, vitamin D and amoxicillin did not show similar harmful effects.

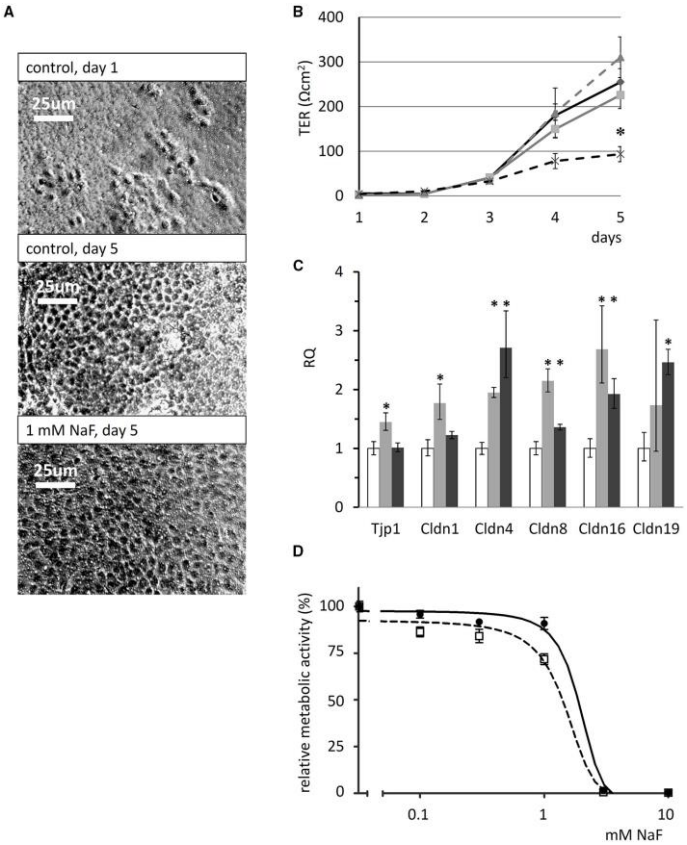

Effects of fluoride on transepithelial resistance, tight-junction protein expression and cell viability of HAT-7 cells. (A) Phase-contrast images of HAT-7 cells grown on Transwell membranes in control medium at day1 and 5 (control), or in the same medium supplemented with 1mM NaF. (B) Transepithelial resistance (TER) of the cells cultured on Transwell membranes for 5 days in the absence (solid black) and presence of 0.3mM (solid gray), 0.6mM (broken gray), or 1mM NaF (broken black line). A significant difference in TER was observed after 5 days when cells cultured with 1mM NaF were compared to controls: *$p < 0.05$. (C) Quantitative RT-PCR data showing expression of tight-junction genes Tjp1, Cldn1, Cldn4, Cldn8, Cldn16, and Cldn19 genes, normalized to mitochondrial Rplpo gene expression in HAT-7 cells treated as described above ($n = 3$ for each gene). Changes in gene expression following treatment with 0.6mM (gray) and 1mM (black) NaF are compared to controls (white): *$p < 0.05$; error bars show 95% confidence intervals. (D) Concentration dependence of the effect of NaF on the metabolic activity of HAT-7 cells treated for 48 h (black circles, continuous line) and 96 h (empty rectangles, broken line) ($n = 6$ for each NaF concentration). (Rácz et al, 2021)

The effects of fluoride 3D ameloblast spheroid formation in the Matrigel matrix were examined in two series of experiments where fluoride at a range of concentrations was added. We found that in the presence of 1 mM fluoride applied from day 4, spheroid size gradually decreased, and by day 7 they were clearly disaggregating. Longer term exposure to 1 mM fluoride, between days 2 and 7, resulted in the formation of only a few small spheroids and significant amounts of cellular debris. 3 mM fluoride killed all HAT-7 cells within 2 days. Exposure to 0.1 and 0.3 mM fluoride for three or six days did not affect spheroid formation compared to controls.

These results support our recent studies on the effect of fluoride using the 2D HAT-7 model, where cells were grown in monolayers on Transwell filters. The delay in tight junction formation observed in the 2D monolayer model also fits well with our finding that HAT-7 spheroids disintegrated after 3 days of exposure to 1mM fluoride when isolated from Matrigel using even the most gentle spheroid isolation procedure. The data indicate that 1 mM fluoride not only affects spheroid formation, but it also weakens the cell-cell adhesion structures responsible of maintaining the spheroid structure.

These findings also highlight the importance of developing a robust and reproducible culture system to investigate questions such as how fluoride alone, or in combination with other environmental stressors, alters enamel formation and biomineralization. Our finding that HAT-

7 cells can form spheroids similar to those formed by primary culture ameloblasts offers the possibility of scaling up this model system to better understand cell-cell and cell-matrix interactions and their importance in enamel formation.

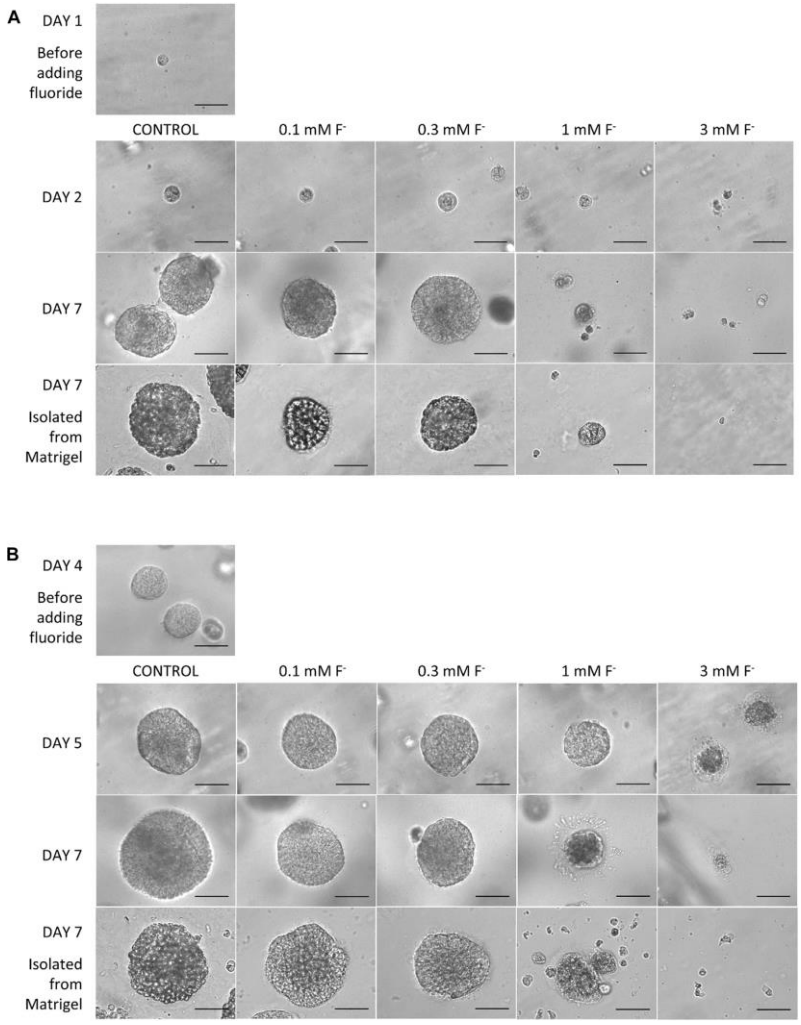

. Morphology of HAT-7 spheroids cultured in Matrigel and Hepato-STIM medium in the absence (control) or presence of fluoride (0.1–3.0 mM). (A) Spheroid images obtained on days 1, 2, and 7 when fluoride (0, 0.1, 0.3, 1.0, 3.0 mM) was added to the culture medium 24 h after seeding. Also shown are spheroids isolated from the Matrigel on day 7. (B) Spheroid images obtained on days 4, 5, and 7 when fluoride (0, 0.1, 0.3, 1.0, 3.0 mM) was added to the culture medium at the time of rapid spheroid growth 4 days after seeding. Also shown are spheroids isolated from the Matrigel on day 7. Scale bars: 70 μm. (Földes et al, 2022)

Translational studies to identify effective treatments to regenerate or repair dental enamel and other oral hard tissues

We have to admit that recent basic science discoveries have not been translated into clinical applications and there is still a long way to go into that direction successfully. Therefore, besides keep working basic science modelling of the physiology and pathophysiology of enamel formation, we also started research on the other end of science: making available clinical results regarding enamel and other oral hard tissue damage for looking optimal procedures to prevent hard tissue damage, and to restore the damaged tissue.

There is a growing need for effective methods in the management of early-stage dental enamel lesions. Therefore, we evaluated the efficacy of combined casein phosphopeptide-amorphous calcium phosphate (CPP-ACP) and fluoride on remineralizing damaged enamel lesions (WSLs) compared to fluoride-only interventions. Our meta-analysis results revealed the combination of the clinically widely used CPP-ACP and fluoride did not overcome the

effect of fluoride given alone. Therefore, more efficient than CPP-ACP are needed to achieve robust enamel remineralization clinically.

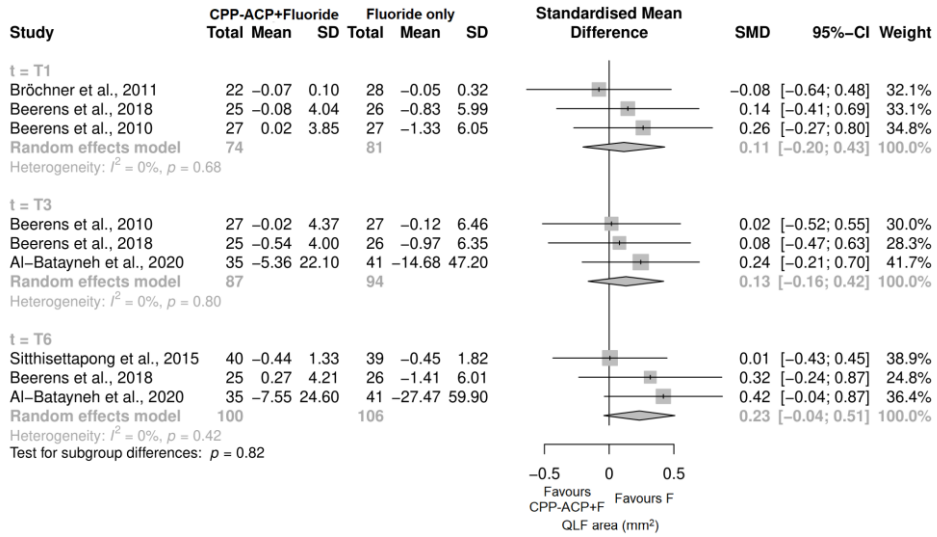

Forest plot of comparison of CPP-ACP + fluoride vs fluoride alone using QLF area (mm2) values difference from baseline and 1, 3 and 6 months of follow-up. CPP-ACP, casein phosphopeptide-amorphous calcium phosphate; QLF, quantitative light-induced fluorescence; SD, standard deviation; MD, mean difference; CI, confidence interval. (Golzio et al, 2022)

In another study we compared the bond failures of different orthodontic materials. This is also important to keep enamel undamaged as much as possible during dental treatment. Our results revealed that RM-GIC had much worse failure rates than acid-etching methods; additionally, the superiority of self-cure resin (SCR) over resin-modified glass ionomer (RM-GIC), indicating strong clinical relevance for preserving enamel.

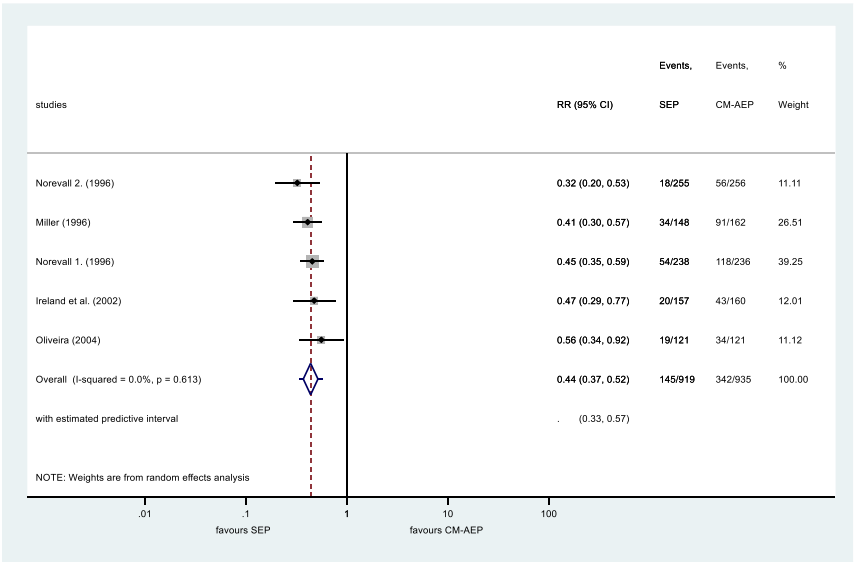

The results showed that in the self-cure resin (SCR) group 15.8% of the brackets failed, whereas in the resin-modified glass ionomer (RM-GIC) group the figure was 36.6%. This great difference means the risk of bracket failure was 56% lower with the SCR technique compared with GIC application. (Dudas et al, 2022)

In cleft lip and palate patients the optimal surgical procedures are important to get the best clinical outcome for all hard tissue in the oral cavity including bone and teeth (i.e. dentin and enamel). Today, the choice between palatoplasty procedures for a complete cleft lip and palate repair is a challenge in the absence of clear guidelines. Therefore, we compared maxillofacial and speech development outcomes after one-stage and two-stage palatoplasties.

Our meta-analysis revealed that the one-stage method may serve as the first choice for operation unless unusual impediments appear in individual cases.

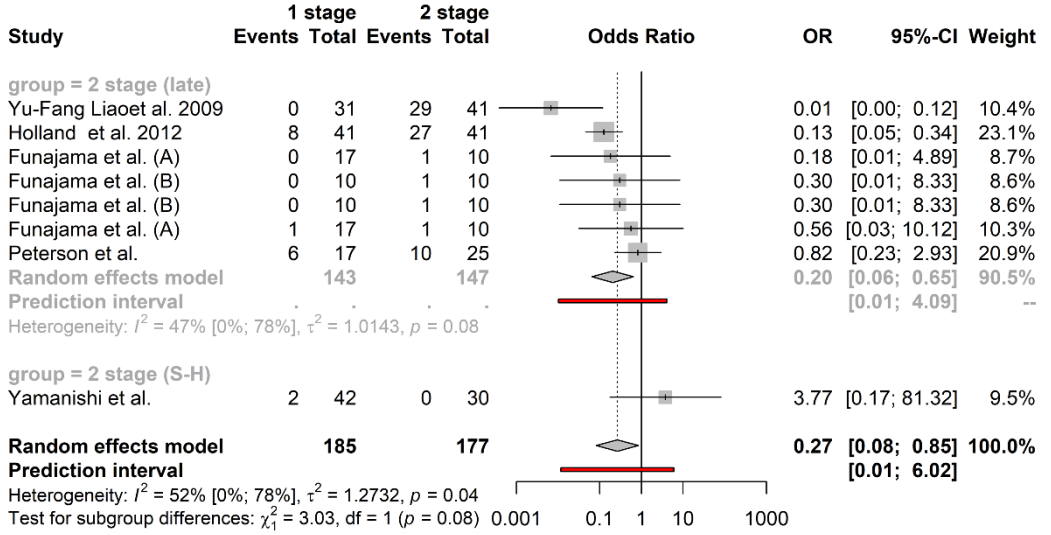

Example Forest plot: Velopharyngeal insufficency**;** (late) delayed two-stage surgery, (S-H) early two stage first soft palate than hard palate; (odds ratio of the event to occur after either one-stage or two-stage surgery) (Schulze-Wennig et al, 2022)

Taken together, these studies will not only provide evidence for basic science and for best clinical practices, but also open the gate not only for basic science directions, but also for new perspectives for clinical applications.

Gábor Varga
Principal investigator